

Testing Method of Alfalfa Seeder Based on High Precision Piezoelectric Sensor

Ying Ma

University of International Business & Economics, Beijing, China

maying@uibe.edu.cn

Keywords: Seeder Experimental Device, Piezoelectric Sensor, Alfalfa Seed, Kalman Filter

Abstract: Alfalfa accounts for about 1/4 of the total area planted in feed crops, it is the main component of feed crops. The development of alfalfa industry can promote the development of aquaculture, processing and trade industries. It not only solves the problem of peasants' employment, but also increases peasants' income, so as to help peasants get rid of poverty and become rich. In conclusion, alfalfa has irreplaceable value and role in agriculture, animal husbandry and economic development. Therefore, it is imperative to select efficient planting and cultivation techniques for alfalfa. The purpose of this paper is to test the alfalfa Seeder Based on High Precision Piezoelectric sensor. An experimental device of Alfalfa Seeder Based on high precision piezoelectric sensor is designed, the device can record the falling of alfalfa seeds in real time. The piezoelectric sensor with precision of 1 mg and 24 $\Delta\Sigma$ modulus converter ADS1256 are used for weighing, the sowing condition of a single alfalfa seed can be distinguished. The sensor uses AMR processor STM32F103C8T6 as the control core, kalman filter algorithm is used to filter the impact of symmetrical weight sensor for seed landing. The simulation and experiment results show that the sensor has high resolution for alfalfa seed sowing and can provide good statistical analysis function.

1. Introduction

Alfalfa, a leguminous plant, is widely cultivated in Eurasia and around the world as an excellent pasture [1]. The cultivation of alfalfa is generally carried out by means of a seeding planter. For example, in northern China, the seeding rate per hectare is 30kg-60kg [2]. However, the alfalfa seeds are very small. In general, the weight of the alfalfa seeds is about 2 g, and the weight of the individual seeds is about 2 mg. The traditional photoelectric seeding sensor is difficult to detect the seeding situation of the seedling in the state of the seeding. For the testing of the seeding device of the seeding machine, a new seeding monitoring sensor and test method are needed. Piezoelectric sensors have high precision, wide measurement range, good evaluation characteristics and long life,

which are very suitable for the measurement of seeding or seeding process of alfalfa seeds [3]. However, the output signal of the sensor is very weak and needs to be modulated and amplified [4-5]. With the development of electronic component technology, $\Delta\Sigma$ analog-to-digital converters have been characterized by high precision and high sampling rate. For example, TI's ADS1256 has a sampling rate of 24 bits and 33K SPS, which can accumulate and weigh the seeding amount of the planter in real time, and obtain the real-time seed sowing condition [6-7].

Piezoelectric vibration acceleration sensors have been widely used in our lives. If there is a large electromagnetic pulse in the environment, electromagnetic pulses will be coupled into the circuit through the power and data lines. Hao studied the electromagnetic pulse protection circuit of the power line and the data line. The protection circuit uses a varistor and a transient suppression tube as transient components. Through simulation, an optimized protection circuit was found. He proposed a method of group comparison. His simulation and experimental results show that his proposed protection circuit can protect the sensor well [8]. Caron's GPS/IMU multi-sensor fusion algorithm introduces context variables to define the fuzzy validity domain of each sensor. The algorithm improves the reliability of location information. Then, the algorithm is simulated by combining the measured GPS and IMU data of a land vehicle. Use context information to detect and reject bad data sent by GPS sensors to improve reliability. In addition, due to the lack of credibility of GPS signals in some cases, and the drift of INS, the current GPS/INS correlation is not satisfactory. In order to avoid this problem, he proposed a fusion process based on multi-sensor Kalman filter to provide acceleration directly by the IMU. In addition, the filter he developed can easily add other sensors to achieve the desired performance [9]. If a system and its observations are represented by linear equations in the state space, the system noise and measurement noise are white, Gaussian, uncorrelated, and the system and measurement noise statistics are accurate; then, the system sequence is the same. The Kalman Filter (KF) provides an optimal state estimate in a simple, fast, and low memory footprint. Since such estimators are of great interest to designers, many linear and nonlinear problems have been solved with KF, and many articles on KF applications appear every year. However, KF is an infinite impulse response (IIR) filter. Therefore, if operating conditions are far from ideal, KF performance can be poor. Researchers in the field of statistical signal processing and control realize that the use of KF faces many problems in practice: insufficient robustness, and the strong influence of temporary uncertainty on initial values, and errors in highly susceptible noise statistics [10].

This paper designs a helium seeder test sensor based on piezoelectric sensor, 24-bit, ultra-low noise analog-to-digital converter ADS1256. The sensor is suitable for the experimental test platform of the hoe planter, and can count the seeding situation of the hoe planter with an output frequency of 10mg and 100Hz. To overcome the impact of seeds falling from a height is the impact of the impact. In this paper, a method of using Kalman filter to overcome the impact interference is proposed. The simulation and experimental results show that the modified sensor has a higher resolution for seeding of alfalfa seeds and can provide good analytical and statistical functions. The innovations of this paper: (1) Analyze and study the working principle of piezoelectric sensor, and carry out temperature calibration experiment to verify that the temperature has a great influence on the accuracy of this type of sensor. In practice, certain measures must be taken. To solve this problem, we can ensure that it has better measurement performance. (2) Software compensation has certain advantages over hardware compensation. This paper proposes the DE-BP model to compensate the temperature of the piezoelectric sensor and compare it with the compensation effect of the traditional BP neural network algorithm. The experimental results show that the DE-BP model has better compensation effect than the traditional BP neural network algorithm for the two static indicators of the sensitivity temperature coefficient and the relative value of the temperature additional error. The relative value of the sensitivity temperature coefficient temperature error can

be the improvement of the temperature compensation model proposed in this paper is verified by an order of magnitude. (3) In order to improve the measurement accuracy and stability of piezoelectric sensors, this paper uses TL431 design circuit to construct a stable constant current source to supply power, and uses curve fitting method to nonlinearly correct it.

2. Proposed Method

2.1. Piezoelectric Sensor

(1) The basic design idea of the piezoelectric sensor is to measure the pressure by the piezoelectric effect of the piezoelectric material, that is, the piezoelectric material is deformed under the action of pressure, and both positive and negative charges are present at both ends of the piezoelectric body. When the applied pressure is within a certain range, the polarization charge generated at both ends of the piezoelectric body is linearly related to the magnitude of the pressure applied to the piezoelectric material, and the pressure value can be calculated according to the amount of charge. Piezoelectric pressure sensors have the advantages of fast response speed and high sensitivity, and are often used to measure pressure signals with large frequency changes. The sensitive component of the piezoelectric sensor is a semiconductor silicon material, which works by utilizing the piezoresistive effect of the semiconductor material to convert a pressure signal that is difficult to measure directly into a voltage signal that is easy to measure. The working principle of a piezoelectric sensor is to utilize the piezoresistive effect of single crystal silicon or polycrystalline silicon. When the piezoresistive effect is subjected to stress along a crystal plane of the semiconductor material, the resistivity changes significantly due to changes in carrier mobility and concentration. The amount of change in resistivity can be expressed as the product of the piezoresistive coefficient and the stress. The piezoresistive effect is widely used in sensors to convert the effects of forces into electrical signal outputs that can be used to measure pressure, stress, strain, velocity, and acceleration. For example, the piezoelectric sensor studied in this paper has a good piezoresistive effect on silicon materials. The pressure is measured in combination with the elastic properties.

(2) The core component of the piezoelectric sensor is a silicon diaphragm located at a central position. The piezoelectric sensor is integrated into the silicon film by a diffusion and integration process to form a silicon piezoresistive chip. The chip is made of a silicon ring. It is fixed inside and connected to the external electrode leads. The inside of the diaphragm is divided into two parts, the lower part is a high pressure chamber, connected to the pressure to be measured, and the lower part is a low pressure chamber, and the atmosphere is open. The four p-type stopbands distributed in the n-type silicon diaphragm are symmetrical with respect to the center of the diaphragm, two of which are located in the compressive stress zone, and the other two are located in the tensile stress zone, which is connected to the Wheatstone bridge structure. When pressure is applied to the silicon diaphragm, the bridge loses balance and produces an electrical signal that is output through the electrode leads.

(3) At present, pressure sensors have been widely used in industrial production, and the basic principle is to utilize the piezoresistive effect of single crystal silicon. Monocrystalline silicon is a very good semiconductor material with a large piezoresistive coefficient. Its single crystal structure can greatly improve the repeatability of the piezoresistive pressure sensor, reduce its hysteresis effect, and allow a wide operating temperature range. With the continuous development of silicon integrated circuit technology, such sensors have been rapidly developed and are widely used in medical inspection, aerospace, safety engineering, geological exploration and other occasions requiring high precision and high sensitivity. Early piezoresistive pressure sensors used bonded strain gauges made of semiconductor material resistors as sensitive components for performance

and stability. With the advancement of related technologies, the industry began to use diffusion processes to form equal-resistance rods in the strained portion of the silicon film. When pressure is applied, the silicon film deforms, which causes the resistance of the strip. When a change occurs, the magnitude of the pressure can be derived from the magnitude of the change. Compared to other types of pressure sensors, silicon sensors have many advantages: high frequency response. Since it does not have any movable unit, it is a whole, so it has a high natural frequency. This feature is very useful for dynamic measurement of the system; it is small and can be miniaturized. At present, the process of integrated circuits is becoming more and more mature, and the silicon diaphragm sensitive components can be made very small, which is very advantageous for miniaturization or miniaturization of pressure sensors; high precision. Since it has no movable structure, there is no friction error when attaching the metal diaphragm or the strain gauge, and there is no error caused by creep or hysteresis, thereby improving the measurement accuracy of the sensor; the sensitivity is high. It is highly sensitive and can meet the needs of most applications. It can be amplified in some cases; stability and reliability are high. It has good stability and is very reliable even in harsh environments. Early Wheatstone bridges were designed to accurately measure voltage. Four resistance strips with equal initial values generated by the resistive elements on the silicon pressure sensitive diaphragm are arranged in the form of a Wheatstone circuit to form a Wheatstone bridge structure. The input voltage can be a constant voltage source or the output voltage is a constant current source. When the diaphragm is not subjected to an external force, the resistance of the resistive element is equal, equal to the initial value, that is, the output voltage is zero at this time, and the bridge is in an equilibrium state. When the diaphragm is subjected to external pressure, the size of the sensitive resistor changes, the bridge loses balance, and the output voltage changes.

2.2. Algorithm Basis of Kalman Filtering

(1) Development of filtering algorithm

The Kalman filter algorithm was first proposed in the mid-20th century. Due to its unique advantages, it has been widely concerned and sought after by the engineering practice community. Kalman filtering combines the theory of estimation and state space theory into two important engineering practice theories, and proposes to abstract the signal transmission process into a linear output process based on Gaussian noise, and it is embodied by the precise design of the equation. Based on the convenience of the input and output relationship and mapping relationship of the dynamic control system, an algorithm based on the system measurement model is obtained. The filtering algorithm and measurement noise are reflected in the estimation process. It is proved that Kalman filtering is effective in one-dimensional variable state estimation. Since the information used in the recursive process is a time domain variable, Kalman filtering still has good performance in the case of multidimensional variables.

Although Kalman filtering has good performance in many industries, even if there is no perfect algorithm in the world, Kalman filtering is no exception, and it needs constant improvement. For the current Kalman filter, he can only be limited to linear systems, while meeting the requirements of Gaussian white noise, and cannot isolate nonlinear non-Gaussian noise. However, in real life, the dynamic systems targeted by industrial applications are mostly nonlinear systems, and some may be strong nonlinear systems, and the system has more or less noise interference. This raises a question for researchers on how to estimate the true value of the state of the system under nonlinear systems.

In the actual research of the development field of filtering algorithms, due to the existence of various uncertain factors, the measurement data has more or less interference, how to obtain more accurate research objects from these data and state information interference information, which is the current A hot topic. In order to reduce the impact of the above interference information,

researchers continue to explore a reasonable data filtering method. When filtering the information, the received interference signal is filtered out as much as possible to extract useful information. In the case of determining the system signal and the interference signal, and the two have different frequency bands, the general filtering (such as RC) network can filter out the noise signal, but in the case where both are random, it needs to be used. Statistical methods provide an optimal estimate of the state of the system. That is to say, the process of filtering the system with a random noise signal is essentially a process of estimating the state of the system.

The development of filtering theory has been relatively long. The least squares method has been widely used in the research field of estimating simple problems. In 1942, American scientists developed and manufactured Wiener filters for air-to-air firing control problems, laying the foundation for solving stochastic control problems based on statistical methods. this is very important. Subsequently, based on Wiener filtering theory, Kalman and Bucy improved the algorithm around 1960 and created a Kalman filter algorithm to overcome the limitations of Wiener filtering. Navigation, control, and tracking fields are widely used. Today, with the rapid development of science and technology, filtering algorithms have a very important research position and irreplaceable role in some fields.

(2) Kalman filter algorithm

Kalman introduced the state variables in the research of filtering theory, and improved the algorithm by recursive method. Finally, Kalman filtering, which is widely praised in the field of automatic control, was established. The basic principle of the Kalman filter algorithm is to estimate the state of the current time of the system according to the state value at the previous moment of the system, obtain the estimated value, and combine the observation value of the current state of the system to estimate the current system state. According to its principle, the Kalman filter algorithm can be divided into two parts: time update and status update. We can use the equation of state of the system:

$$X_k = AX_{k-1} + BU_k + W_k \quad (1)$$

And the measurement equation of the system node:

$$Z_k = HK_k + V_k \quad (2)$$

To represent the system. In the formula, X_{k-1} indicates the state of the system at time k-1, and U_k indicates the amount of control applied to the system at time k. A and B are parameters of the system state. For a system with multiple models, they are matrices. Z_k is the measured value of the research object at time k, and H is the corresponding parameter in the system measurement process. When the measurement system has multiple variables, H is a matrix. W_k and V_k are the process noise of the system and the measurement noise of the system, respectively. They are all assumed to be Gaussian white noise (the instantaneous value obeys the Gaussian distribution of noise), and Q and R are used to represent the covariance of the two.

According to the recursive principle of Kalman filter algorithm, we can predict the state of the current time (K time) of the system according to the optimal estimation value \hat{X}_{k-1} at a moment (time k-1) of the system, and obtain the one-step prediction value $\hat{X}_{k,k-1}$ of the state. the formula is as follows:

$$\hat{X}_{k,k-1} = A\hat{X}_{k-1} + BU_k \quad (3)$$

Similarly, a one-step prediction of the systematic error covariance P can be obtained. The formula is as follows:

$$P_{k,k-1} = AP_{k-1}A' + Q \quad (4)$$

In formula (4), A' is the transposition of A , and equations (3) and (4) are the time update equations of Kalman filter.

With the prediction results $\hat{X}_{k,k-1}$ and $P_{k,k-1}$ of the current time (k time) state, combined with the measured values of the system k time state, we can optimize the state of the system k time to obtain the optimal estimation value \hat{X}_k , the formula is as follows:

$$\hat{X} = \hat{X}_{k,k-1} + Kg_k(Z_k - H\hat{X}_{k,k-1}) \quad (5)$$

Where Kg_k is the Kalman gain and can be calculated by equation (6).

$$Kg_k = \frac{P_{k,k-1}H'}{(HP_{k,k-1}H' + R)} \quad (6)$$

In order to keep the Kalman filter running, we also need to update the error covariance P at system k . The formula is as follows:

$$P_k = (1 - Kg_k H)P_{k,k-1} \quad (7)$$

Equation (5), formula (6) and formula (7) constitute the state update equation of Kalman filter.

The flow chart of the Kalman filter algorithm is shown in Figure 1. When running the Kalman filter algorithm, the initial values of each parameter must be set first, and the initial values of different parameter values are set, which will be the Kalman filter algorithm. The treatment effect has a significant impact, and the results of the impact results will be compared in Chapter 4. After the initial value is determined, the Kalman filter begins to work. Based on the given initial value of the state, one-step prediction of the state and error covariance is performed using equations (3) and (4), and a one-step prediction based on the error covariance. Combine the formula (6) to find the current Kalman gain. By taking the obtained Kalman gain into the formula (5), the current time can be obtained, and the optimal estimation value of the object state is studied, and the optimal estimation of the error covariance at this moment is updated to complete a cycle. operating. Next, the optimal state and error covariance estimate at the current time is taken as the initial value of the next cycle, and the next round of calculation is performed until the end of the iteration.

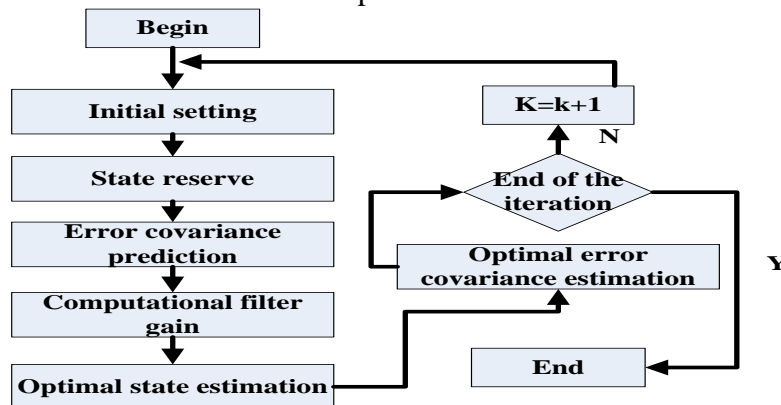


Figure 1. Kalman filter algorithm flow chart

2.3. Principle of Nonlinear Correction

In general, we characterize the static characteristics of a system through input and output characteristics. It is also one of the important indicators that determine the measurement accuracy of a measurement system. In an ideal environment, the mapping relationship between the input and output of the piezoelectric sensor should be linear, but it can be seen from the experiments in Chapter 2 that the static characteristics of the sensor are not linear and are compared with the ideal environmental deviation big. Therefore, we need to make nonlinear correction of the output of the piezoelectric sensor to realize the linear output of the measurement system, generally in two ways: hardware circuit correction and software method. However, in modern intelligent measurement systems, because the types of sensors used are very rich and their nonlinear characteristics are different, it is undoubtedly a lot of work to design a hardware circuit for each sensor to correct the output curve. And cost input, so this paper uses software to complete the nonlinear correction of the piezoelectric sensor, that is, the intelligent straight line fitting of the sensor output results in a linear relationship between input and output.

3. Experiments

3.1. Experimental Tools

In this experiment, the sensor control core adopts AMR processor STM32F103C8T6 and piezoelectric sensor device with weighing accuracy of 10mg, and ADS1256 device with 24-bit $\Delta\Sigma$ analog-to-digital converter that can distinguish single seed hoe seeding. In order to detect the influence of temperature on the piezoelectric sensor, the temperature of the working environment is monitored by the integrated temperature sensor model AD590 provided in the THSRZ-2 experimental device. Integrated Temperature Sensor the AD590 is manufactured by Analog Devices, Inc., and is essentially a monolithic integrated current source with temperature sensing. Because its output current is proportional to temperature, it is often used to measure temperature. The AD590's temperature range is $-55\text{ }^{\circ}\text{C}$ - $150\text{ }^{\circ}\text{C}$, which is suitable for most industrial production environments. It has a simple peripheral circuit and stable measurement performance, so it is widely used.

3.2. Experimental Design and Data Collection

The AD590 temperature sensor used in this design produces a stable current when the temperature is constant. It functions like a constant current source and has good linearity. Therefore, only need to add a power supply to achieve a linear conversion of temperature to current, in order to measure the temperature, add a sampling resistor at the terminal to measure its voltage value. The temperature sensor AD590 has its output voltage amplified and then measured to avoid errors caused by inaccurate readings due to too small output.

Piezoelectric sensors are made from the piezoresistive effect of semiconductor materials, and their measurement results are susceptible to temperature and error. When the temperature rises, the piezoresistive coefficient of the semiconductor material will decrease. When the temperature decreases, the piezoresistive coefficient will increase. Therefore, the resistance of the resistor bar will be affected by the temperature, so that the measurement of the piezoelectric sensor is not Accurate, there is a phenomenon of temperature drift, referred to as temperature drift. In order to correct the measurement error caused by the temperature drift of the piezoelectric piezoelectric sensor in the later research, this paper conducts a calibration experiment to measure the output voltage value at different temperatures. Figure 2 below shows the data acquisition process in the

seeding experiment.

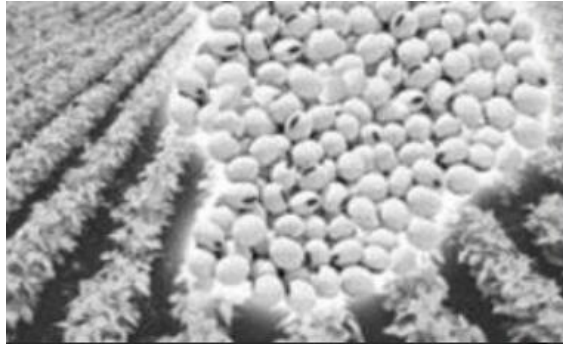


Figure 2. Soybean experimental data collection

4. Discussion

4.1. Piezoelectric Sensor Application Environment Analysis

The output voltage of the temperature sensor is recorded as $U(v)$ at different ambient temperatures, and the output voltage of the piezoresistive pressure sensor is U_p . Because the piezoresistive pressure sensor has small input pressure and small output voltage under laboratory conditions, in order to reduce the error caused by reading, the measurement results are amplified. The measurement results are shown in Table 1:

Table 1. Experimental data for piezoelectric sensors

| T (°C) | U (V) | 10 | 20 | 30 | 40 | 50 | 60 | 70 | 80 | 90 | 100 |
|--------|-------|-------|-------|-------|-------|-------|-------|-------|-------|-------|-------|
| 15.1 | U_p | 0.15 | 0.286 | 0.391 | 0.518 | 0.518 | 0.628 | 0.715 | 0.815 | 0.92 | 1.463 |
| | U_t | 0.191 | 0.221 | 0.221 | 0.231 | 0.231 | 0.222 | 0.191 | 0.181 | 0.211 | 0.212 |
| 17.7 | U_p | 0.149 | 0.284 | 0.397 | 0.513 | 0.614 | 0.723 | 0.808 | 0.903 | 0.993 | 1.054 |
| | U_t | 0.317 | 0.327 | 0.354 | 0.285 | 0.287 | 0.285 | 0.288 | 0.295 | 0.287 | 0.229 |
| 19.3 | U_p | 0.187 | 0.274 | 0.388 | 0.503 | 0.615 | 0.717 | 0.805 | 0.886 | 0.97 | 1.05 |
| | U_t | 0.363 | 0.353 | 0.253 | 0.263 | 0.363 | 0.263 | 0.363 | 0.363 | 0.363 | 0.363 |
| 21.6 | U_p | 0.155 | 0.268 | 0.379 | 0.496 | 0.495 | 0.558 | 0.696 | 0.777 | 0.953 | 1.133 |
| | U_t | 0.469 | 0.458 | 0.446 | 0.466 | 0.546 | 0.556 | 0.446 | 0.656 | 0.676 | 0.666 |
| 23.6 | U_p | 0.152 | 0.254 | 0.373 | 0.486 | 0.583 | 0.68 | 0.778 | 0.847 | 0.934 | 1.013 |
| | U_t | 0.516 | 0.516 | 0.516 | 0.516 | 0.516 | 0.516 | 0.516 | 0.516 | 0.516 | 0.516 |
| 25.1 | U_p | 0.144 | 0.252 | 0.367 | 0.478 | 0.584 | 0.681 | 0.774 | 0.843 | 0.931 | 1.001 |
| | U_t | 0.591 | 0.591 | 0.591 | 0.591 | 0.591 | 0.591 | 0.591 | 0.591 | 0.591 | 0.581 |
| 27 | U_p | 0.195 | 0.335 | 0.341 | 0.368 | 0.482 | 0.552 | 0.652 | 0.733 | 0.801 | 0.903 |
| | U_t | 0.266 | 0.362 | 0.326 | 0.336 | 0.356 | 0.365 | 0.466 | 0.768 | 0.815 | 0.961 |

In this paper, the relative values of sensitivity temperature coefficient and temperature additional error are selected as the performance indicators for measuring the measurement accuracy of piezoresistive pressure sensors. The sensitivity temperature coefficient indicates the speed of sensitivity drift with temperature, and is numerically equal to the percentage change of sensitivity when the temperature changes by 1 degree Celsius; the relative value of temperature additional error is the maximum degree of non-coincidence between the static characteristic of the

measurement system and a fixed straight line.

Using a piezoelectric sensor and placing it at different ambient temperatures for calibration experiments, the input and output values are recorded. It can be seen that the voltage values of the outputs are not equal when the ambient temperature is different and the input pressure is the same. Through the input and output relationships at different temperatures plotted in MATLAB, it is verified that the piezoresistive pressure sensor is susceptible to temperature, resulting in temperature drift. And the data of the calibration experiment is analyzed, and the sensitivity temperature coefficient is $8.4808 \times 10^{-3} / ^\circ\text{C}$ and the relative value of the temperature additional error is 32.3120%, which indicates that the accuracy of the data measured by the piezoelectric sensor is poor, so the electric sensor is made. Temperature compensation is very necessary.

4.2. Temperature Compensation Analysis

According to the data in Table 1, the curve fitting of the experimental calibration data by LSLAB is carried out in MATLAB. It can be concluded that the output characteristic curve of the piezoresistive pressure sensor is shown in Figure 3 under different operating temperatures.

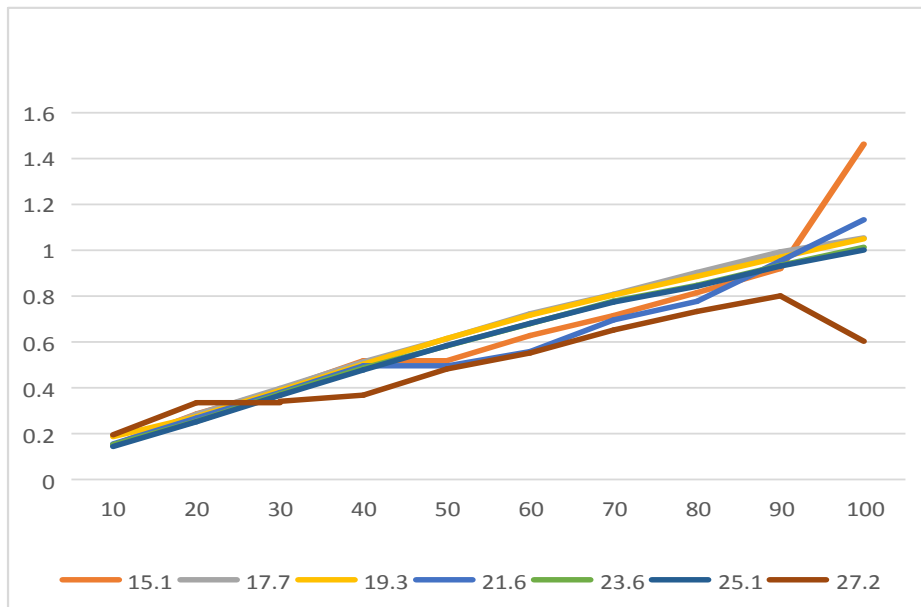


Figure 3. Fitted line graph before compensation

It can be seen from Fig. 2 that the characteristic curve of the piezoelectric sensor is not the same when operating at different ambient temperatures. In other words, when the temperature changes, the output voltage of the piezoelectric sensor changes with temperature. For example, when the input pressure of the piezoelectric sensor is 10 kPa, the outputs are: 0.160 V (20.1 °C), 0.159 V (28.7 °C), 0.157 V (36.3 °C), 0.155 V (44.6 °C), and 0.152 V (51.6 °C), 0.144V (59.1 °C), 0.135V (66.0 °C), that is, the temperature has an influence on the output of the piezoelectric sensor, making the measurement result unstable, so it is necessary to compensate the temperature of the piezoelectric sensor.

4.3. Analysis of the Influence of Power Supply Stability on the Bridge

The Wheatstone bridge inside the piezoelectric sensor is shown in Figure 4. The terminals 1 and 3 are the inputs of the bridge, and the ends 2 and 4 are the outputs of the bridge. When the bridge is

in an equilibrium state, the initial resistances of the four sensitive resistors are equal and both, that is, the output voltage is zero at this time. When the diaphragm is subjected to external stress, the resistance of the sensitive resistor will change, and the bridge will be out of equilibrium, resulting in a change in the output voltage from the purpose of measuring the pressure. As can be seen from the above description, the output voltage of the piezoresistive pressure sensor is closely related to the bridge resistance and the power supply. If the power supply is improperly selected, the stability of the output voltage will be affected, thereby greatly reducing the piezoresistive pressure sensor. The performance of the work, so choosing the right power supply is critical.

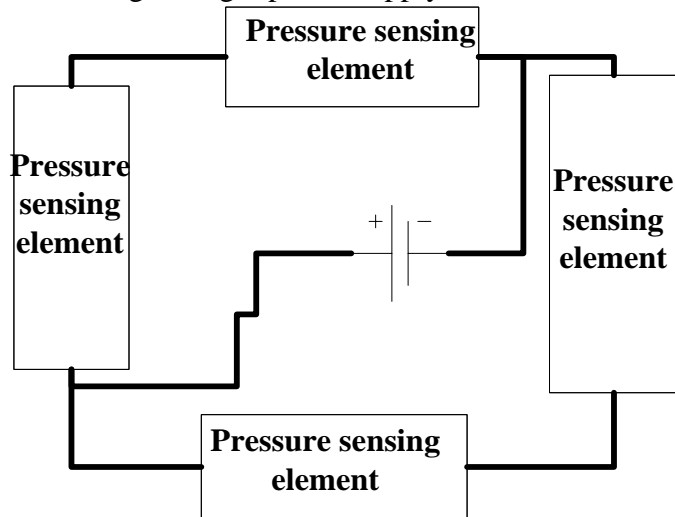


Figure 4. Wheatstone bridge structure

4.4. Nonlinear Correction Error Analysis

According to the improved PauTa criterion, the residual error U is calculated as [0.5, 0.6, 0.6, 0.6, 0.8, 0.5, 2.3, 0.6, 2.5, 0.6], respectively, where the coarse errors of the sensors with serial numbers 7 and 9 are too large, judged as Outliers are removed. The remaining 8 groups of residual errors are less than $1.5U$, so they are regarded as valid data. Before the next fusion, the two outliers need to be cleared. Then weighted average fusion is used, and the corresponding optimal weighting factors W_i are:

[0.125, 0.125, 0.094, 0.107, 0.150, 0.150, 0.094, 0.150] The fusion result was $X = 17.4$ Pa.

Using the same fusion process, the combined humidity was 65% (65.069%) and the soil moisture was 73% (73.272%). According to the specific measurement value brought into $G+C1V1+C2V2+C3V3$, it is calculated that the level of water to be added is 1.01 (because the number of acres in the alfalfa planting area is undetermined, the amount of irrigation here is in units of level). At the same time, since the temperature and humidity are not above or below the warning range, there is no need to turn on the fan, heater, humidifier and dehumidifier. The experimental results using this decision system and the arithmetic mean method are shown in Figure 5:

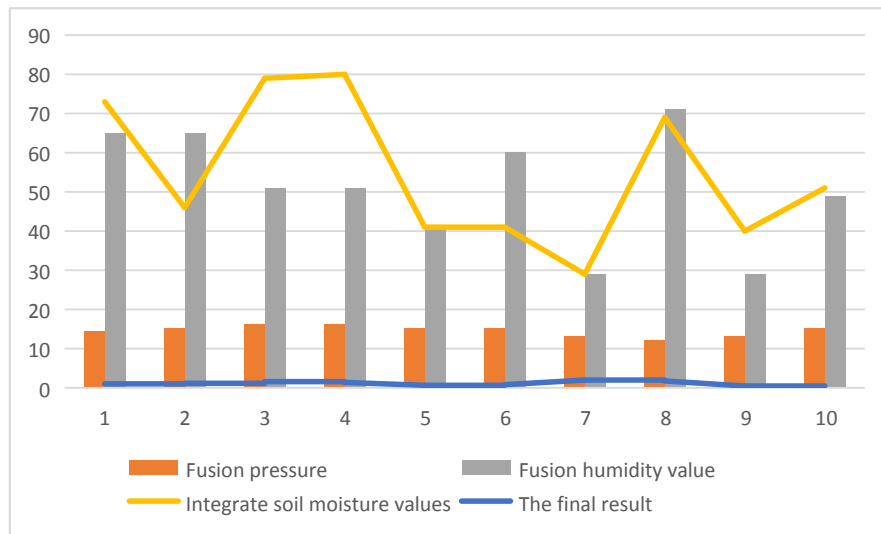


Figure 5. Comparison of experimental data

If the system algorithm is not used to process the data, only the arithmetic mean is obtained, and multi-source fusion is not used. Taking the pressure value as an example, the obtained result is shown in Fig. 6.

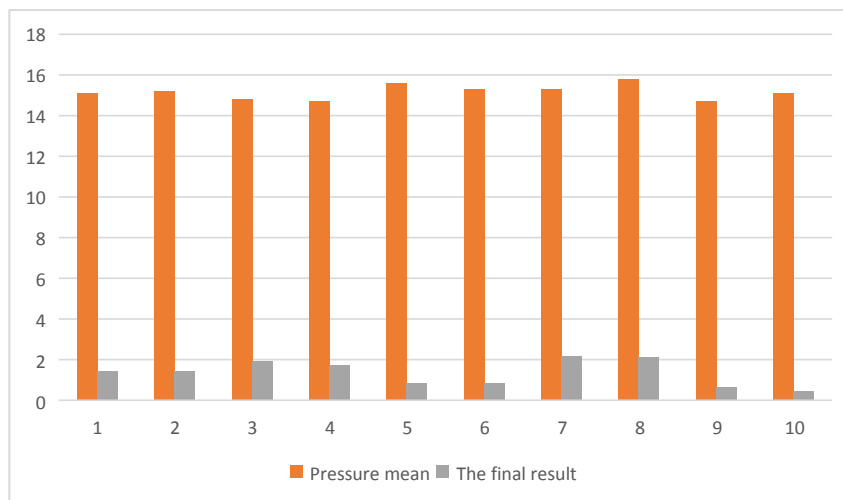


Figure 6. Experimental data using only arithmetic mean

Taking the experimental data as an example: the average pressure is 15.1 Pa, and the accuracy of the obtained environmental parameters is lower than the experimental results. The amount of water added is then determined by a single environmental parameter and the results are 1.42. The final result of adding water is also far from the results of this experiment. It can be seen from the data results that the data fusion method can improve the measurement accuracy of the sensor and effectively eliminate the error caused by the sensor failure. Through the use of multi-source fusion technology, the irrigation capacity of irrigation equipment is more accurately divided, and the combined operation of multiple devices is realized, and the stability and reliability of the system are also improved. The calibration experimental data is averaged and made in the MATLAB software, as shown in Figure 7.

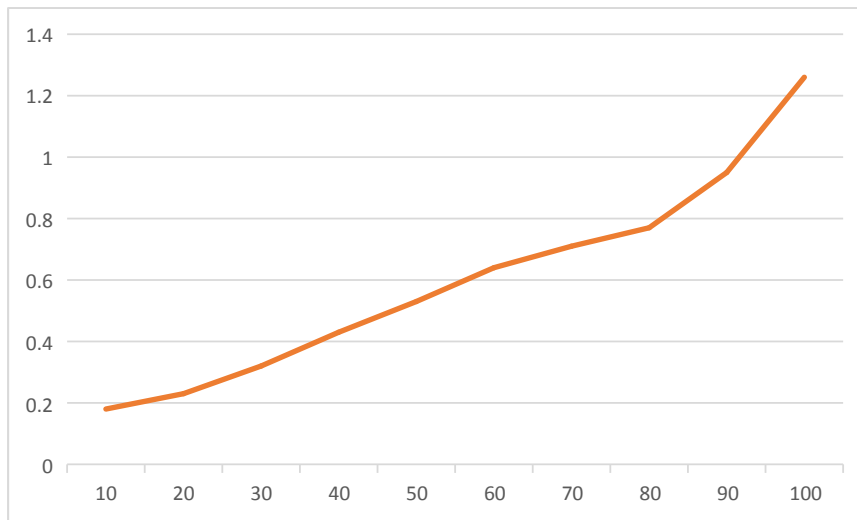


Figure 7. Input and output characteristics before nonlinear correction

According to the linearity calibration data, the inverse model of the piezoresistive pressure sensor can be established. After the nonlinear calibration of the calibration data of the piezoresistive pressure sensor, the linearity of the system is greatly improved.

5. Conclusion

This paper mainly introduces several factors that may reduce the measurement accuracy of piezoelectric sensors and proposes corresponding solutions. The first is to use TL431 to design a precision constant current source to supply the piezoelectric sensor. Then, the DE-BP model is used to fuse the measurement results of the piezoelectric sensor, and the data before and after the fusion is analyzed. The performance index of the sensor has been greatly improved, which proves that the DE-BP model proposed in this paper can effectively reduce the influence of temperature on the piezoelectric sensor. Finally, the output of the piezoelectric sensor is obtained by curve fitting. The characteristic curve is nonlinearly corrected to improve linearity.

Piezoelectric sensors are made of semiconductor materials because they are inherently susceptible to temperature and do not guarantee the stability of measurement accuracy. Therefore, this paper designs a smart seeding monitoring system, which consists of STM32F103 microcontroller, piezoelectric sensor, temperature sensor and designed peripheral circuit to form a complete system, based on DE-BP model to suppress the adverse effects of ambient temperature. It is nonlinearly corrected using curve fitting. The actual experimental results show that the temperature compensation algorithm proposed in this paper is feasible and has good compensation effect, and the designed measurement system is stable in operation, reliable in performance and relatively low in cost.

The research object of this paper is piezoelectric sensor. The purpose is to design an intelligent seeding monitoring system, which uses software to compensate its temperature and use curve fitting to perform nonlinear correction to maximize the stability of its working performance. Due to the limitations of my research and laboratory conditions, there are still many aspects to be improved, such as: (1) the dynamic characteristics of the sensor are also worth studying, but this paper only considers the static characteristics of the sensor. In the future, we can try the artificial intelligence algorithm. Combine the two to improve the performance of the sensor; (2) This paper communicates directly with the PC through the RS232 interface. In the future, a low-power Bluetooth module can be introduced for communication, which is convenient for engineering

applications. The temperature compensation algorithm proposed in this paper needs further research and Optimization will further improve the impact of temperature on the performance of the pressure sensor, and will continue to explore other forms of temperature compensation algorithms in the future and fully optimize the system.

Funding

This article is not supported by any foundation.

Data Availability

Data sharing is not applicable to this article as no new data were created or analysed in this study.

Conflict of Interest

The author states that this article has no conflict of interest.

References

- [1] Pan, M., Li, R., Xu, L., Yang, J., Cui, X., & Wang, S. (2018) "Reproducible molecularly imprinted piezoelectric sensor for accurate and sensitive detection of ractopamine in swine and feed products", *Sensors*, 18(6), pp.1870. DOI: 10.3390/s18061870
- [2] Armanious, G., & Lind, R. (2017) "Fly-by-Feel Control of an Aeroelastic Aircraft using Distributed Multirate Kalman Filtering", *Journal of Guidance Control & Dynamics*, 40(9), pp.1-7.
- [3] Fariz, N., Jamil, N., & Din, M. M. (2018) "An Improved Indoor Location Technique Using Kalman Filtering on Rssi" *Journal of Computational & Theoretical Nanoscience*, 24(3), pp.1591-1598. DOI: 10.1166/asl.2018.11116
- [4] Shi, W., Wang, Y., & Wu, Y. (2017) "Dual Mimic Pedestrian Navigation by Inequality Constraint Kalman Filtering", *Sensors*, 17(2), pp.427.
- [5] Xu, S. K., Hong, X. F., Cheng, Y. B., Liu, C. Y., Li, Y., & Yin, B.(2018) "Validation of a piezoelectric sensor array-based device for measurement of carotid-femoral pulse wave velocity: the philips prototype", *Pulse*, 5(1-4), pp.161-168.
- [6] Bit Lee, H., Kim, Y. W., Yoon, J., Lee, N. K., & Park, S. H. (2017) "3d customized and flexible tactile sensor using a piezoelectric nanofiber mat and sandwich-molded elastomer sheets", *Smart Material Structures*, 26(4), pp.045032.
- [7] Dionelis, N., & Brookes, M. (2018) "Phase-Aware Single-Channel Speech Enhancement with Modulation-Domain Kalman Filtering", *IEEE/ACM Transactions on Audio Speech & Language Processing*, 26(5), pp.937-950.
- [8] Hao, C., & Li, D. (2018) "Electromagnetic Pulse Protection of Piezoelectric Vibration Acceleration sensor", *Ferroelectrics*, 535(1), pp.1-7.
- [9] Caron, F., Duflos, E., Pomorski, D., & Vanheeghe, P. (2006) "Gps/imu Data Fusion Using Multisensor Kalman Filtering: Introduction of Contextual Aspects", *Information Fusion*, 7(2), pp.221-230. DOI: 10.1016/j.inffus.2004.07.002
- [10] Shmaliy, Y. S., Zhao, S., & Ahn, C. K. (2017) "Unbiased Finite Impulse Response Filtering: an Iterative Alternative to Kalman Filtering Ignoring Noise and Initial Conditions", *IEEE Control Systems*, 37(5), pp.70-89.